A growth factor signaling cascade confined to circular ruffles in macrophages

Timothy P. Welliver[1] and Joel A. Swanson[1,2,*]

[1]Program in Immunology and [2]Department of Microbiology and Immunology, University of Michigan Medical School, Ann Arbor, MI 48109-5620, USA

*Author for correspondence (jswan@umich.edu)

Biology Open 1, 754–760
doi: 10.1242/bio.20121784
Received 30th April 2012
Accepted 23rd May 2012

Summary

The formation of macropinosomes requires large-scale movements of membranes and the actin cytoskeleton. Over several minutes, actin-rich surface ruffles transform into 1–5 μm diameter circular ruffles, which close at their distal margins, creating endocytic vesicles. Previous studies using fluorescent reporters of phosphoinositides and Rho-family GTPases showed that signals generated by macrophages in response to the growth factor Macrophage Colony-Stimulating Factor (M-CSF) appeared transiently in domains of plasma membrane circumscribed by circular ruffles. To address the question of how signaling molecules are coordinated in such large domains of plasma membrane, this study analyzed the relative timing of growth factor-dependent signals as ruffles transformed into macropinosomes. Fluorescent protein chimeras expressed in macrophages were imaged by microscopy and quantified relative to circular ruffle formation and cup closure. The large size of macropinocytic cups allowed temporal resolution of the transitions in phosphoinositides and associated enzyme activities that organize cup closure. Circular ruffles contained transient and sequential spikes of phosphatidylinositol (4,5)-bisphosphate ($PI(4,5)P_2$), phosphatidylinositol (3,4,5)-trisphosphate (PIP_3), diacylglycerol, $PI(3,4)P_2$, PI(3)P and the activities of protein kinase C-α, Rac1, Ras and Rab5. The confinement of this signal cascade to circular ruffles indicated that diffusion barriers present in these transient structures focus feedback activation and deactivation of essential enzyme activities into restricted domains of plasma membrane.

Key words: Macropinocytosis, Phosphoinositides, Signal transition

Introduction

Macropinocytosis is an actin-based movement of the cell surface leading to ingestion of extracellular fluid. During macropinosome formation, the actin cytoskeleton reshapes membrane topography, initially through the formation of cell surface ruffles. Some ruffles curve to form circular ruffles, also known as macropinocytic cups, which then close into plasma membrane-derived intracellular vacuoles (Swanson, 2008). Macropinocytosis mediates antigen sampling by dendritic cells and provides a mechanism of cell invasion by some viruses and bacteria (Mercer and Helenius, 2009; Swanson and Watts, 1995). It occurs constitutively in many cells, including many cancer cells, and in other cells after stimulation with growth factors or phorbol esters (Kerr and Teasdale, 2009).

This study examines the mechanisms which coordinate signaling chemistry with ruffling, ruffle closure into cups and cup closure into macropinosomes. Macropinocytosis and the trafficking of many membranous organelles are regulated by membrane phosphoinositides (PIs) in the cytoplasmic leaflet of the membrane bilayer (Di Paolo and De Camilli, 2006). PIs recruit cytoplasmic proteins or activate membrane-associated enzymes with specific PI-binding domains, thereby organizing membrane-associated chemistries locally (DiNitto and Lambright, 2006; Krauß and Haucke, 2007). Species of PI which affect macropinocytosis include phosphatidylinositol (PtdIns) (4,5)-bisphosphate ($PI(4,5)P_2$), PtdIns (3,4,5)-trisphosphate (PIP_3), PtdIns (3,4)-bisphosphate ($PI(3,4)P_2$), and PtdIns 3-phosphate (PI(3)P). Enzymes which phosphorylate, dephosphorylate or hydrolyze PIs are essential to ruffling and macropinocytosis. Synthesis of $PI(4,5)P_2$ by phosphatidylinositol 4-phosphate 5-kinase (PI4P5K) at the plasma membrane can increase actin polymerization (Krauß and Haucke, 2007). $PI(4,5)P_2$ can be phosphorylated to PIP_3 by phosphatidylinositol 3-kinase (PI3K) type I or hydrolyzed by phospholipase C-γ (PLCγ) to inositol 1,4,5-trisphosphate (IP_3) and diacylglycerol (DAG). PI3K and PLCγ act sequentially during macropinocytosis in Src-transformed cells (Amyere et al., 2000). DAG in membranes recruits and activates Protein Kinase C (PKC) (Azzi et al., 1992), which regulates actin polymerization (Apgar, 1995; Hartwig et al., 1992). The inositol 5-phosphatase SHIP-1 can dephosphorylate PIP_3 to yield $PI(3,4)P_2$, which may be further dephosphorylated by PI 4′-phosphatases to PI(3)P (Ivetac et al., 2005). PI(3)P is also synthesized from PtdIns by PI3K type III (Fruman et al., 1998).

The versatility of PIs as signaling molecules relates partly to the diversity of proteins and activities they regulate. Prominent among these are small GTPases, which regulate a wide variety of cellular activities through effector enzymes. GTPases implicated in macropinocytosis include Rac1 (Jaffe and Hall, 2005), Ras (Bar-Sagi and Feramisco, 1986), Rab5 (Feliciano et al., 2011; Lanzetti et al., 2004), Cdc42 (Garrett et al., 2000), Arf6 (Donaldson et al., 2009), Rab34 (Sun et al., 2003) and RhoG

(Ellerbroek et al., 2004). Formation of circular ruffles and macropinosomes entails a sequence of interdependent regulatory interactions between GTPase-dependent effector pathways. For example, Ras and PI3K act upstream of Rac and Rab5, leading to circular ruffle formation (Lanzetti et al., 2004) and Rab5 regulates increases in Rac1 signaling on forming macropinosomes (Palamidessi et al., 2008). However, these interactions do not yet comprise a coherent model of how cytoplasmic chemistry is organized to build a macropinosome.

Signal dynamics can be imaged by fluorescence microscopy of reporter molecules expressed in living cells and applied to large scale movements of phagocytosis and macropinocytosis. During Fc receptor-mediated phagocytosis, distinct chemical transitions are evident during early and late stages of phagosome formation. The initial movements of phagocytosis and the advancing edge of the developing phagocytic cup contain high concentrations of $PI(4,5)P_2$, PIP_3, and active Cdc42, Rac1 and Arf6 (Beemiller et al., 2006; Botelho et al., 2000; Hoppe and Swanson, 2004; Vieira et al., 2001). Later during cup formation, especially at the base of the cup, concentrations of the early signals decrease and levels of DAG, PKCε, active Rac2, Rac1 and Arf1 increase (Beemiller et al., 2006; Botelho et al., 2000; Hoppe and Swanson, 2004).

PI3K is necessary for completion of both Fc receptor-mediated phagocytosis and M-CSF-stimulated macropinocytosis. The PI3K inhibitors wortmannin and LY294002 do not inhibit ruffling or phagocytic cup formation, but instead inhibit contractile activities that close phagosomes and macropinosomes into the cell (Amyere et al., 2000; Araki et al., 1996; Swanson et al., 1999). This indicates that the products of PI3K are required for the later stages of cup closure. Consistent with a role for PI3K in organizing late stages of phagosome formation, transitions from early to late signals were shown to be regulated by PI3K and by concentrations of 3′PIs in the cup (Beemiller et al., 2006; Zhang et al., 2010). Imaging studies of macrophages responding to the growth factor M-CSF identified two signaling nodes during macropinosome formation. PIP_3 and Rac1-GTP appeared transiently in macropinocytic cups soon after ruffle closure (Welliver et al., 2011; Yoshida et al., 2009). These spikes of PIP_3 and Rac1 activation were confined to circular ruffles and preceded the gradual accumulation of PI(3)P and Rab5a, which peaked about the time of cup closure. The correlation between ruffle closure and the spikes of PIP_3 and Rac1 indicated that signal amplification in large subdomains of plasma membrane is conditional on morphological transitions; i.e., the formation of the circular ruffle (Yoshida et al., 2009). As ruffles and macropinocytic cups can limit lateral diffusion of membrane proteins (Welliver et al., 2011) and phagocytic cups contain barriers to diffusion of $PI(4,5)P_2$ (Golebiewska et al., 2011), we hypothesize that the spatial organization provided by restricted lateral mobility permits localized organization of signaling cascades in cup domains of plasma membrane. The large size of macropinosomes allowed us to analyze how signaling nodes are organized during macropinosome morphogenesis. Using live cell fluorescence microscopy to visualize signals generated in murine bone marrow-derived macrophages (BMM) in response to M-CSF, we quantified essential signals relative to the component stages of macropinosome formation. We report that circular ruffles confine transient, sequential spikes of signaling activities, which include transitions between PtdIns isoforms and associated activities of Rac1, Ras, Rab5 and PKCα.

Results

Because signaling correlates with morphological stages of macropinocytosis, and macropinosomes form at various times after growth factor addition (Yoshida et al., 2009), we used visual markers of the process to compare the timing of different signals. Ruffle closure, identified by phase-contrast microscopy, was used to align macropinocytic events from different video sequences. To relate the timing of Rab5 localization to cup closure, we localized CFP-MEM and mCherry-Rab5 by 4-dimensional fluorescence microscopy. Expression of CFP-MEM allowed visualization of plasma membrane morphology during macropinocytosis. The 4-D imaging indicated that Rab5 localized to forming macropinocytic cups and reached peak intensities after macropinosomes had closed into the cell (Fig. 1A).

The timing of cup closure relative to Rab5 localization was determined by FM4-64 photobleaching experiments. FM4-64 is a lipophilic dye that, when added to culture medium, labels the outer leaflet of exposed membrane surfaces. As its fluorescence is negligible in water, membranes can be visualized in the continuous presence of dye (Yoshida et al., 2009). FM4-64 has low photostability, causing it to bleach quickly under epifluorescence illumination. In cell membranes exposed to dye-containing medium, bleached molecules are rapidly replaced by non-bleached molecules. In a closed macropinosome with a limited supply of FM4-64 molecules, photobleaching depletes the fluorescent molecules enclosed in the macropinosome, leading to decreased fluorescence. Hence, the inflection point of FM4-64 fluorescence intensity vs. time indicates the point of cup closure (i.e., macropinosome isolation from the external medium). We measured FM4-64 photobleaching by ratiometric imaging of BMM expressing CFP-MEM and Citrine-Rab5. The inflection point in FM4-64/CFP-MEM ratios, marking cup closure, occurred 100 s after ruffle closure (Fig. 1B,C), consistent with earlier observations (Yoshida et al., 2009). Citrine-Rab5/CFP-MEM ratios increased continuously in macropinocytic cups, beginning just after ruffle closure and peaking 80 sec after the FM4-64 inflection point (i.e., 180 sec after ruffle closure) (Fig. 1B,D).

The consistent intervals between ruffle closure and maximal Rab5 recruitment allowed the timing of other signals to be measured relative to the stages of macropinosome formation. PI and DAG levels were measured by ratiometric imaging of cells expressing the CFP and Citrine-chimeras of various lipid-binding domains, including Citrine-PLCδ1PH to localize $PI(4,5)P_2$ (Botelho et al., 2000; Lemmon et al., 1995), Citrine-BtkPH to localize PIP_3 (Rameh et al., 1997; Várnai et al., 1999), Citrine-Tapp1PH to localize $PI(3,4)P_2$ (Dowler et al., 2000; Kamen et al., 2007), Citrine-2xFYVE to localize PI3P (Gillooly et al., 2000; Henry et al., 2004) and Citrine-C1δ to localize DAG (Botelho et al., 2000; Oancea et al., 1998). Each of these probes concentrated in macropinocytic cups. Moreover, the timing of their peak localization varied and revealed patterns of PI modification. A spike of $PI(4,5)P_2$ localization followed 20 sec after ruffle closure (Fig. 2A; supplementary material Movie 1). At the end of the spike, Citrine-PLCδ1PH/CFP ratios dropped below the initial levels, indicating depletion of $PI(4,5)P_2$ from cup membranes. The PIP_3 spike followed the $PI(4,5)P_2$ spike (Fig. 2B,E; supplementary material Movie 1), indicating phosphorylation of $PI(4,5)P_2$ by PI3K type I. Similarly, the pattern of Citrine-Tapp1PH recruitment indicated that $PI(3,4)P_2$

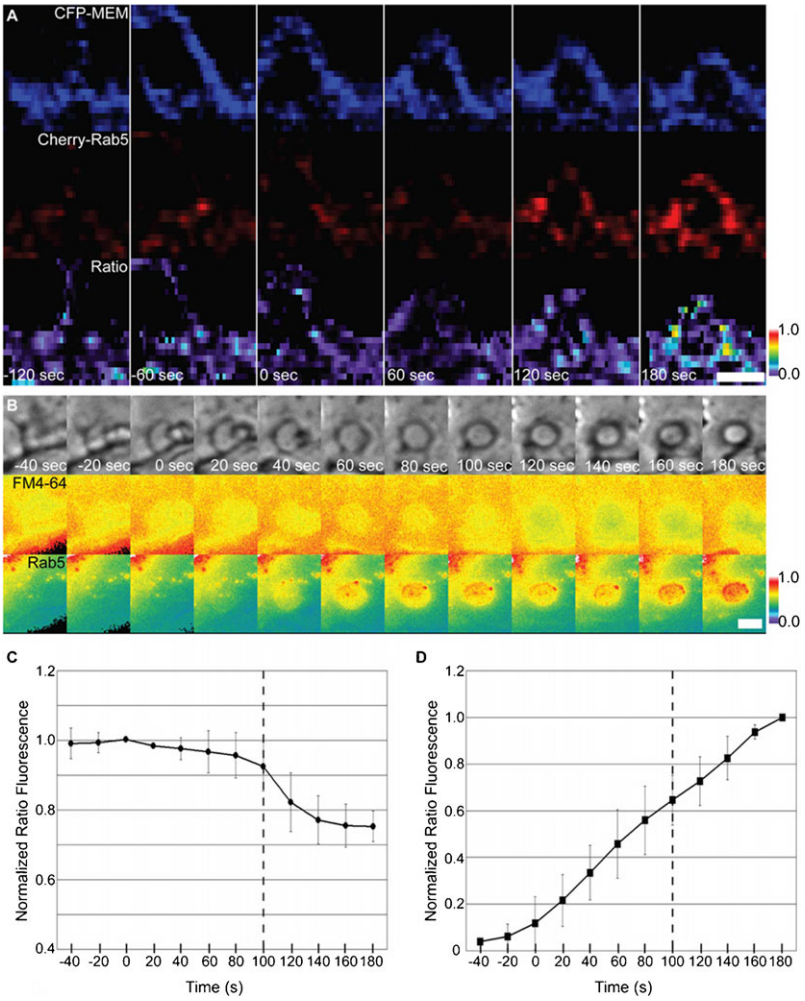

Fig. 1. Macropinosome closure precedes peak localization of Rab5. (**A**) 4D reconstruction of Cherry-Rab5 localization during macropinocytosis. Through-focus z-stacks of CFP-MEM and mCherry-Rab5 at regular intervals during M-CSF-stimulated macropinocytosis, showing distribution of CFP-MEM (blue, top row), Cherry-Rab5 (red, middle row) and Cherry/CFP ratio (pseudocolor). Time points are separated by 60 s; "0 s" marks the point of cup closure. Rab5 localization increased after complete cup closure. (**B–D**) The timing of cup closure relative to Rab5 localization. (B) Macrophages expressing CFP-MEM and Citrine-Rab5 were imaged in 1 µg/ml FM4-64. Top row: phase-contrast; middle row: intensity of ratiometric FM4-64/CFP-MEM; bottom row: Citrine-Rab5/CFP-MEM ratio. Ruffle closure occurred at *t=0*. FM4-64 photobleaching increased at *t=100 s*, indicating cup closure. Scale bars = 3.0 µm. (C) Plot of ratiometric FM4-64/CFP-MEM intensity during macropinosome formation; the inflection point occurred at *t=100 s*. (D) Plot of Cit-Rab5/CFP-MEM ratios during macropinosome formation. Rab5 localization peaked at *t=180 s*, after macropinosome closure. Error bars indicate standard deviation. $n \geqslant 9$ for each curve.

concentrations peaked as PIP_3 concentrations were declining, roughly coincident with cup closure (Fig. 2C,E; supplementary material Movie 1). In contrast to the sharp transient increases in $PI(4,5)P_2$, PIP_3 and $PI(3,4)P_2$, the concentrations of PI(3)P increased gradually and coincidently with Rab5, beginning just after ruffle closure and peaking after $PI(3,4)P_2$ concentrations decreased (Fig. 2D,E; supplementary material Movie 1). DAG concentrations peaked shortly after the disappearance of $PI(4,5)P_2$ and coincident with the peak of PIP_3, indicating that $PI(4,5)P_2$ was concurrently converted to DAG and PIP_3 in cups (Fig. 3A,D; supplementary material Movie 1). Overall, the patterns observed by ratiometric imaging indicated three courses of PI conversion in cups: (a) PI(4)P to $PI(4,5)P_2$ to PIP_3 to $PI(3,4)P_2$ to PI(3)P, (b) PI(4)P to $PI(4,5)P_2$ to DAG and IP_3 and (c) a prolonged synthesis of PI(3)P, likely from PI.

Enzymes relevant to macropinocytosis showed variable localization in cups. Citrine-PLCγ1 localized to cups throughout macropinosome formation (Fig. 3B). Citrine-PKCα localized to cups following the spike of DAG, in patterns resembling those for Cherry-Rab5 and PI(3)P (Fig. 3C,D). Unlike phagocytosis (Larsen et al., 2002; Zhang et al., 2010), YFP-PKCε did not localize to macropinocytic cups (data not shown).

GTPase activities were measured relative to ruffle closure and Rab5 localization. Endogenous Rac1 activity was localized using a Citrine chimera of the p21-binding domain (PBD) of Pak1, which binds to GTP-bound Rac1 (Edwards et al., 1999; Hoppe and Swanson, 2004). As noted previously, ratiometric localization of YFP-PBD indicated peak Rac1 activation coincident with the PIP_3 spike (Fig. 4A,C) (Yoshida et al., 2009). Peak Ras activation, measured by ratiometric localization of Citrine-labeled Ras-binding domain (RBD), occurred after the PIP_3 spike (Fig. 4B,C), approximately concurrent with localization of Rab5. This indicated that Ras is active on macropinosomes at the early endosome-like stage, consistent with earlier studies (Porat-Shliom et al., 2008). The dynamics of Ras and Rab5 were not monitored more than 180 sec after ruffle closure.

Thus, the patterns of labeling in cups revealed two distinct signaling nodes organizing macropinosome formation: PIP_3/DAG/Rac1, peaking 60–80 sec after ruffle closure, and PI(3)P/PKCα/Ras, reaching maximal levels after cup closure. Moreover, the PIP_3 spike was bracketed by spikes of $PI(4,5)P_2$, $PI(3,4)P_2$ and PI(3)P, indicating the flow of phosphate in the signaling cascade.

Discussion

This study identified a sequence of signals that occur during macropinosome formation, most strikingly in the clear spatiotemporal organization of PI modifications that underlie

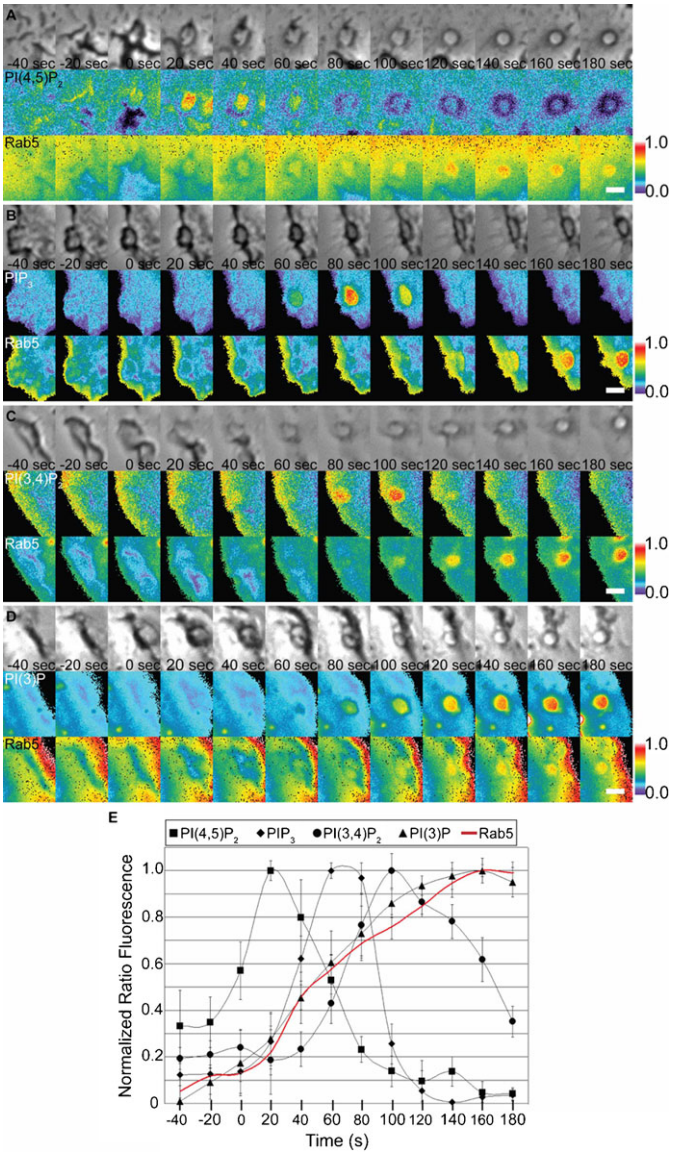

Fig. 2. Fluorescence imaging of phosphoinositide localization during macropinocytosis. (**A–D**) Macrophages expressing mCerulean, mCherry-Rab5, and Citrine-tagged probes for PIs were imaged during M-CSF-stimulated macropinocytosis. Top rows: phase-contrast; middle rows: Citrine-tagged fluorophore/mCerulean ratios; bottom rows: mCherry-Rab5/mCerulean ratios. Ruffle closure occurred at *t=0*. Scale bars = 3.0 µm. (A) Citrine-PLCδ1PH peaked at *t=20 s*. (B) Citrine-BtkPH peaked at *t=80 s*. (C) Citrine-Tapp1PH peaked at *t=100 s*. (D) Citrine-FYVE peaked at *t=180 s*. (**E**) Plot of compiled data comparing relative timing of peak labeling by different PI probes. Error bars indicate standard deviation. $n \geqslant 9$ for each condition.

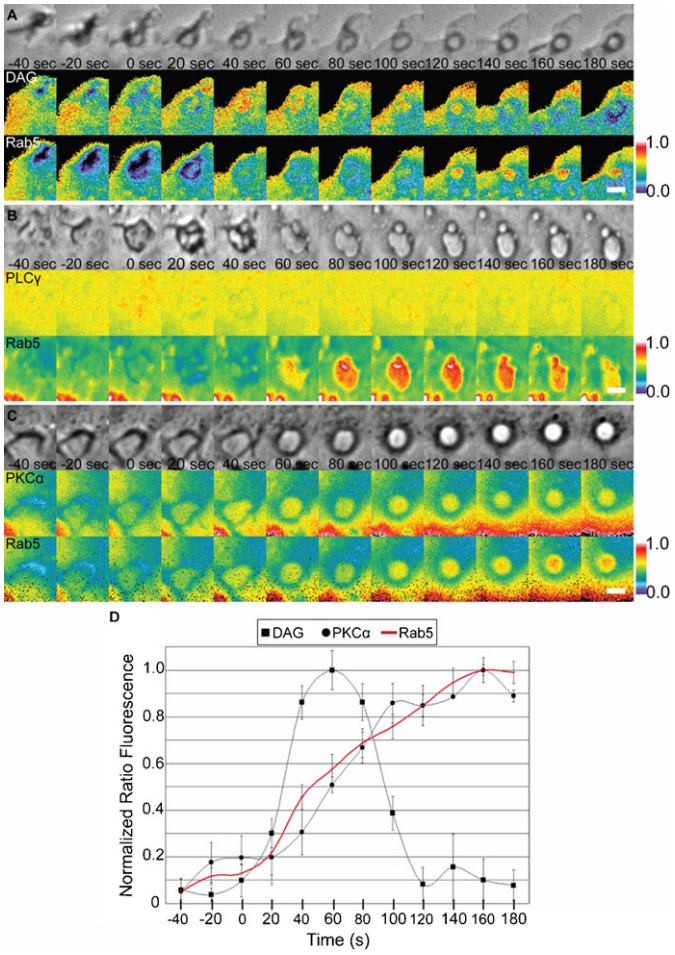

Fig. 3. Fluorescence imaging of the DAG pathway during macropinocytosis. (**A–C**) Macrophages expressing mCerulean, mCherry-Rab5, and Citrine-tagged probes were imaged during macropinocytosis. For each panel: top row = phase-contrast, middle row = ratio of Citrine-tagged fluorophore/mCerulean, bottom row = ratio of mCherry-Rab5/mCerulean. Ruffle closure occurred at *t=0*. Scale bars = 3.0 µm. (A) Citrine-C1δ peaked at *t=60 s*. (B) Citrine-PLCγ did not demonstrate differential localization during macropinocytosis. (C) Citrine-PKCα localization peaked at *t=180 s*, resembling localization patterns of Rab5. (**D**) Relative timing of signaling in the DAG pathway. $n \geqslant 9$ for each curve. Error bars indicate standard deviation.

the PIP_3 spike. Two major signaling nodes appeared in circular ruffles (Fig. 5). The first, a spike in Rac1 activity, PIP_3 and DAG, appeared in a large subdomain of plasma membrane created by ruffle closure. The second, a slower rise in the activities of PKCα, Ras, Rab5, and PI(3)P, began in the open cup and peaked shortly after cup closure. The transition between these two signaling nodes was confined to these isolated regions of plasma membrane.

The timing of PI spikes indicated coordinated chemical transformations inside macropinocytic cups. PtdIns (4)-phosphate (PI(4)P), the likely substrate in the synthesis of $PI(4,5)P_2$, is widely distributed in the plasma membrane (Di Paolo and De Camilli, 2006). $PI(4,5)P_2$ concentrations were high in ruffles but increased after ruffle closure, suggestive of a positive feedback amplification of PI4P5K in cups. As $PI(4,5)P_2$ concentrations decreased, concentrations of PIP_3 and DAG increased, indicating concurrent activities of PI3K and PLCγ1. The depletion of $PI(4,5)P_2$ continued until its levels fell below pre-spike levels. Similarly, PIP_3 and DAG concentrations decreased to negligible levels following their transient increases. This suggests that the PIP_3 spike could be explained by changing enzyme activities and substrate concentrations in cups. Accordingly, increased $PI(4,5)P_2$ concentrations provide substrate for PIP_3 synthesis by PI3K, PIP_3 activates PLCγ1 and PI3K to generate DAG and more PIP_3, respectively, producing a rapid localized increase in PIP_3 concentration. The continued action of PLCγ1 and PI3K deplete $PI(4,5)P_2$ in the cup, slowing PIP_3 synthesis. Finally, PIP_3 is depleted by dephosphorylation to $PI(3,4)P_2$.

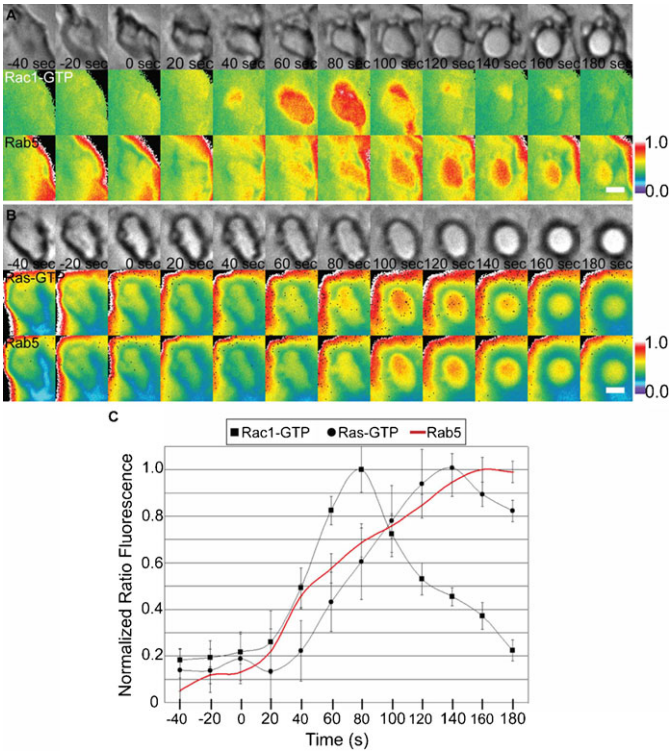

Fig. 4. Imaging of GTPase activity during macropinocytosis. (**A**,**B**) Macrophages expressing mCerulean, mCherry-Rab5, and either mCitrine-PBD, a probe for Rac1-GTP, or mCitrine-RBD, a probe for Ras-GTP, were imaged during macropinocytosis. Top rows: phase-contrast; middle rows: Citrine-tagged fluorophore/mCerulean ratio; bottom rows: mCherry-Rab5/mCerulean ratio. *t=0* indicates ruffle closure. Scale bars = 3.0 μm. Color bars indicate relative intensities of ratio images. (A) Citrine-PBD localization peaked at *t=80 s*. (B) Citrine-RBD peaked at *t=180 s*. (**C**) Quantitation showed that peak activation of Rac1 occurred at *t=80 s*. Ras reached maximal activation at t=*180 s*. $n \geqslant 9$ for each condition.

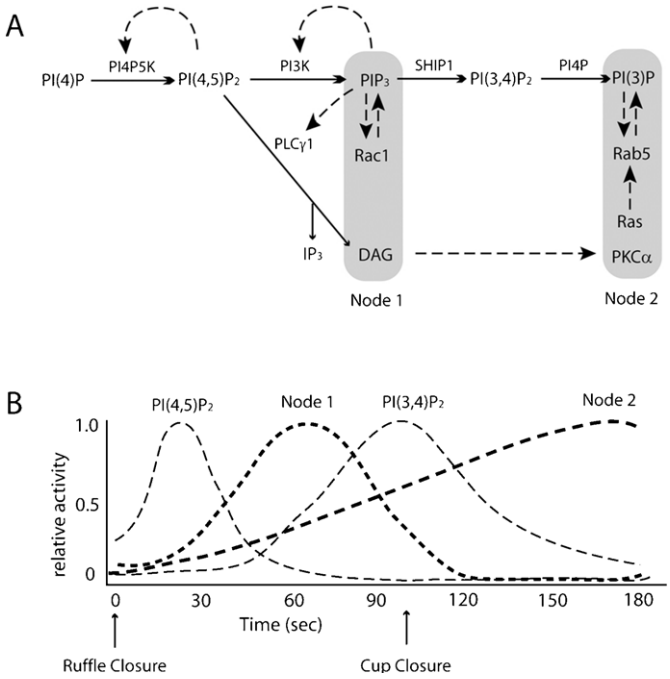

Fig. 5. Summary of the signal cascade in circular ruffles. The sequence of chemical transformations occurring between the formation of a fully circular ruffle and the closure of the circular ruffle into the cell as a macropinosome begins with an increase in $PI(4,5)P_2$. (**A**) Chemical changes in cups. Solid lines with small arrowheads indicate precursor-product relationships. Hatched lines with large arrowheads indicate activation pathways enhanced inside circular ruffles. The spike of $PI(4,5)P_2$ is followed by increases of PIP_3, DAG and the activity of Rac1 (Node 1), and later by a transient increase of $PI(3,4)P_2$. The levels of PI(3)P and the activities of Ras, Rab5 and PKCα (Node 2) increase continuously in the cup, peaking after cup closure and the transient increases of $PI(4,5)P_2$, PIP_3, DAG and $PI(3,4)P_2$. (**B**) The timing of signals in cups relative to Ruffle Closure and Cup Closure.

These studies also revealed the dynamics of GTPase activities relative to the PI transitions. Coincident accumulation of PIP_3 and activation of Rac1 suggested that these molecules contribute to a feedback amplification mechanism. Cherry-Rab5 recruitment to cups began just after ruffle closure, consistent with roles for Rab5 in Rac delivery into cup domains (Palamidessi et al., 2008) and in stabilizing circular ruffles (Lanzetti et al., 2004). Maximal Ras activation appeared later than maximal DAG accumulation, consistent with models in which Ras is activated by PKCα or DAG and signals on formed endosomes (Hancock, 2003; Porat-Shliom et al., 2008).

Circular ruffles circumscribe relatively large regions of plasma membrane – much larger than other known spatially organized domains for receptor signaling, such as lipid rafts (Prior et al., 2003) or signaling complexes (Kholodenko et al., 2010). Circular ruffles limit diffusion of membrane proteins out of cups (Welliver et al., 2011), and the present findings suggest they also confine lipids to cup domains. Barriers to diffusion of $PI(4,5)P_2$ were identified in phagocytic cups (Golebiewska et al., 2011), which are structurally analogous to macropinocytic cups. Thus, barriers that limit molecular egress by lateral diffusion can define signaling domains that restrict enzymatic reactions to subregions of the cell surface. This leads to spatially focused transitions of PIs which integrate GTPase-dependent effector pathways on cup membranes. Accordingly, these transitions of regulatory molecules would lead to transitions in the cytoskeletal movements necessary for macropinosome closure.

As diffusion barriers, membrane ruffles could facilitate local feedback activation and inhibition of lipid-modifying chemistries. Signal amplification by restricted diffusion would require PI concentration-dependent feedback amplification. For example, absent barriers, PIP_3 produced by locally activated PI3K would diffuse laterally in the plasma membrane from its site of synthesis and remain at concentrations below the thresholds for downstream signaling. Diffusion barriers that confine PIP_3 could allow its concentrations to increase near their sites of synthesis to levels that activate positive feedback activation of PI3K and increased synthesis of PIP_3. Feedback activation of PI3K by PIP_3 could occur via Gab2 (Gu et al., 2003) or Gab1 (Rodrigues et al., 2000).

In many of the mechanisms in which PI chemistry organizes cell morphology, such as in phagocytosis and chemotaxis, PIs and GTPases cooperatively activate effector proteins to organize cell structure (Di Paolo and De Camilli, 2006). This work indicates a complementary dynamic, in which cell structure itself organizes lipid-modifying chemical reactions. Assembly of plasma membrane subdomains defined by circular ruffles precedes receptor-dependent signal amplification, deactivation and transitions to later signals. This indicates that

macropinocytosis is a self-organized chemical process, the beginning of which is conditional on formation of the circular ruffle.

Materials and Methods

Cell culture

Bone marrow-derived macrophages (BMMs) were generated as described previously (Knapp and Swanson, 1990; Swanson, 1989). Bone marrow exudate was obtained from femurs of C57BL/6J mice and cultured in medium (DMEM with 20% FBS and 30% L cell-conditioned medium) promoting the differentiation of macrophages. Bone marrow cultures were differentiated for 1 week with additions of fresh differentiation medium at days 3 and 6. Macrophages were transfected using Amaxa Nucleofector II, protocol Y-01, and plated onto 25-mm circular coverslips. Plasmid constructs included Citrine-PLCδ1PH (Botelho et al., 2000; Lemmon et al., 1995), Citrine-BtkPH (Rameh et al., 1997; Várnai et al., 1999), Citrine-Tapp1PH (Dowler et al., 2000; Kamen et al., 2007), Citrine-2xFYVE (Gillooly et al., 2000; Henry et al., 2004), Citrine-C1δ (Botelho et al., 2000; Oancea et al., 1998) and mCherry-Rab5 (Feliciano et al., 2011). Cultures were incubated overnight in medium lacking M-CSF (RPMI 1640 with 20% heat-inactivated FBS). All experiments were performed the day after transfection. All imaging experiments were temperature controlled at 37℃.

Microscopy

Phase-contrast and fluorescence images were collected at 20 sec intervals in a Nikon Eclipse TE-300 inverted microscope with a 60× numerical aperture 1.4, oil-immersion PlanApo objective lens (Nikon, Tokyo, Japan) and a Lambda LS xenon arc lamp for epifluorescence illumination (Sutter Instruments, Novato, CA, USA). Fluorescence excitation and emission wavelengths were selected using a JP4v2 filter set (Chroma Technology, Rockingham, VT) and a Lambda 10-2 filter wheel controller (Shutter Instruments) equipped with a shutter for epifluorescence illumination control. Images were recorded with a Photometrics CoolSnap HQ cooled CCD camera (Roper Scientific, Tucson, AZ, USA). Cells were first imaged in Ringer's Buffer (155 mM NaCl, 5 mM KCl, 2 mM $CaCl_2$, 1 mM $MgCl_2$, 2 mM NaH_2PO_4, 10 mM glucose and 10 mM HEPES at pH 7.2), then 200 ng/mL M-CSF (R&D Systems) in Ringer's buffer was added to stimulate macropinocytosis. Image acquisition and processing were performed using MetaMorph v6.3 (Molecular Devices, Sunnyvale, CA, USA).

Ratiometric imaging

Ratiometric imaging was used to correct for variations in optical path length caused by cell morphology. Specifically, fluorescence intensities for images of a fluorescent chimera were divided by fluorescence intensities of a non-chimeric fluorescent marker of cell volume (e.g. Ceramide) or plasma membrane (CFP-MEM). All ratiometric images were generated using MetaMorph processing software.

FM4-64 microscopy experiments

FM4-64 (1 μg/mL) in Ringer's buffer was applied to cells expressing CFP-MEM and YFP-Rab5. Images were collected every 20 seconds, with 1 second exposures, using a 555-nm excitation filter and a 605-nm emission filter.

Fluorescence intensity measurements

Measurements of fluorescence intensities were made using the "draw region" and "region measurement" tools of Metamorph. For each macropinosome, measurements were collected starting two frames (−40 s) before the frame showing ruffle closure (0 s). Measurements were collected until after Rab5 had reached its peak intensity, typically around 180 s after ruffle closure.

For each condition, the average fluorescence of the entire cell was subtracted from experimental readings, removing baseline signal. Comparison of the timing of different signaling events relied on normalizing signals to their peak intensities during macropinosome formation. Peak intensity was the highest measured fluorescence ratio during a sequence. Fluorescence ratios at all timepoints of a series were divided by the peak intensity to obtain a normalized fluorescence ratio that indicated the strength of a signal relative to that molecule's peak intensity. The peak intensity therefore indicated the time at which that signaling molecule was most prevalent relative to ruffle closure.

4D reconstruction microscopy

Cells expressing CFP-MEM and mCherry-Rab5 fluorophores were imaged using an Olympus FV-500 Confocal microscope fitted with a 100× 1.45 NA oil immersion objective. The microscope was equipped with argon (for CFP imaging), and HeNe green (for mCherry imaging) lasers. Image collection used Fluoview FV500 imaging software. Image Z-stacks used a step size of 250 nm between planes. Images were collected continuously in line sequential scanning mode.

Image stacks were deconvolved using Huygens Essential (Scientific Volume Imaging, Hilversum, Netherlands). Resulting images were reconstructed into 4D image stacks. Ratiometric image stacks of mCherry-Rab5/CFP-MEM were created using MetaMorph. Stacks were visualized using the 4D viewer and linescan function in MetaMorph.

Acknowledgements

The authors thank Dr. Samuel Straight for technical advice and assistance. This research was supported by National Institutes of Health [AI-079414 to J.A.S.].

Competing Interests

The authors have no competing interests to declare.

References

Amyere, M., Payrastre, B., Krause, U., Van Der Smissen, P., Veithen, A. and Courtoy, P. J. (2000). Constitutive macropinocytosis in oncogene-transformed fibroblasts depends on sequential permanent activation of phosphoinositide 3-kinase and phospholipase C. *Mol. Biol. Cell* **11**, 3453-3467.

Apgar, J. R. (1995). Activation of protein kinase C in rat basophilic leukemia cells stimulates increased production of phosphatidylinositol 4-phosphate and phosphatidylinositol 4,5-bisphosphate: correlation with actin polymerization. *Mol. Biol. Cell* **6**, 97-108.

Araki, N., Johnson, M. T. and Swanson, J. A. (1996). A role for phosphoinositide 3-kinase in the completion of macropinocytosis and phagocytosis by macrophages. *J. Cell Biol.* **135**, 1249-1260.

Azzi, A., Boscoboinik, D. and Hensey, C. (1992). The protein kinase C family. *Eur. J. Biochem.* **208**, 547-557.

Bar-Sagi, D. and Feramisco, J. R. (1986). Induction of membrane ruffling and fluid-phase pinocytosis in quiescent fibroblasts by ras proteins. *Science* **233**, 1061-1068.

Beemiller, P., Hoppe, A. D. and Swanson, J. A. (2006). A phosphatidylinositol-3-kinase-dependent signal transition regulates ARF1 and ARF6 during Fcγ receptor-mediated phagocytosis. *PLoS Biol.* **4**, e162.

Botelho, R. J., Teruel, M., Dierckman, R., Anderson, R., Wells, A., York, J. D., Meyer, T. and Grinstein, S. (2000). Localized biphasic changes in phosphatidylinositol-4,5-bisphosphate at sites of phagocytosis. *J. Cell Biol.* **151**, 1353-1368.

Di Paolo, G. and De Camilli, P. (2006). Phosphoinositides in cell regulation and membrane dynamics. *Nature* **443**, 651-657.

DiNitto, J. P. and Lambright, D. G. (2006). Membrane and juxtamembrane targeting by PH and PTB domains. *Biochim. Biophys. Acta* **1761**, 850-867.

Donaldson, J. G., Porat-Shliom, N. and Cohen, L. A. (2009). Clathrin-independent endocytosis: a unique platform for cell signaling and PM remodeling. *Cell. Signal.* **21**, 1-6.

Dowler, S., Currie, R. A., Campbell, D. G., Deak, M., Kular, G., Downes, C. P. and Alessi, D. R. (2000). Identification of pleckstrin-homology-domain-containing proteins with novel phosphoinositide-binding specificities. *Biochem. J.* **351**, 19-31.

Edwards, D. C., Sanders, L. C., Bokoch, G. M. and Gill, G. N. (1999). Activation of LIM-kinase by Pak1 couples Rac/Cdc42 GTPase signalling to actin cytoskeletal dynamics. *Nat. Cell Biol.* **1**, 253-259.

Ellerbroek, S. M., Wennerberg, K., Arthur, W. T., Dunty, J. M., Bowman, D. R., DeMali, K. A., Der, C. and Burridge, K. (2004). SGEF, a RhoG guanine nucleotide exchange factor that stimulates macropinocytosis. *Mol. Biol. Cell* **15**, 3309-3319.

Feliciano, W. D., Yoshida, S., Straight, S. W. and Swanson, J. A. (2011). Coordination of the Rab5 cycle on macropinosomes. *Traffic* **12**, 1911-1922.

Fruman, D. A., Meyers, R. E. and Cantley, L. C. (1998). Phosphoinositide kinases. *Annu. Rev. Biochem.* **67**, 481-507.

Garrett, W. S., Chen, L.-M., Kroschewski, R., Ebersold, M., Turley, S., Trombetta, S., Galán, J. E. and Mellman, I. (2000). Developmental control of endocytosis in dendritic cells by Cdc42. *Cell* **102**, 325-334.

Gillooly, D. J., Morrow, I. C., Lindsay, M., Gould, R., Bryant, N. J., Gaullier, J.-M., Parton, R. G. and Stenmark, H. (2000). Localization of phosphatidylinositol 3-phosphate in yeast and mammalian cells. *EMBO J.* **19**, 4577-4588.

Golebiewska, U., Kay, J. G., Masters, T., Grinstein, S., Im, W., Pastor, R. W., Scarlata, S. and McLaughlin, S. (2011). Evidence for a fence that impedes the diffusion of phosphatidylinositol 4,5-bisphosphate out of the forming phagosomes of macrophages. *Mol. Biol. Cell* **22**, 3498-3507.

Gu, H., Botelho, R. J., Yu, M., Grinstein, S. and Neel, B. G. (2003). Critical role for scaffolding adapter Gab2 in FcγR-mediated phagocytosis. *J. Cell Biol.* **161**, 1151-1161.

Hancock, J. F. (2003). Ras proteins: different signals from different locations. *Nat. Rev. Mol. Cell Biol.* **4**, 373-385.

Hartwig, J. H., Thelen, M., Rosen, A., Janmey, P. A., Nairn, A. C. and Aderem, A. (1992). MARCKS is an actin filament crosslinking protein regulated by protein kinase C and calcium-calmodulin. *Nature* **356**, 618-622.

Henry, R. M., Hoppe, A. D., Joshi, N. and Swanson, J. A. (2004). The uniformity of phagosome maturation in macrophages. *J. Cell Biol.* **164**, 185-194.

Hoppe, A. D. and Swanson, J. A. (2004). Cdc42, Rac1, and Rac2 display distinct patterns of activation during phagocytosis. *Mol. Biol. Cell* **15**, 3509-3519.

Ivetac, I., Munday, A. D., Kisseleva, M. V., Zhang, X. M., Luff, S., Tiganis, T., Whisstock, J. C., Rowe, T., Majerus, P. W. and Mitchell, C. A. (2005). The type Iα

inositol polyphosphate 4-phosphatase generates and terminates phosphoinositide 3-kinase signals on endosomes and the plasma membrane. *Mol. Biol. Cell* **16**, 2218-2233.

Jaffe, A. B. and Hall, A. (2005). Rho GTPases: biochemistry and biology. *Annu. Rev. Cell Dev. Biol.* **21**, 247-269.

Kamen, L. A., Levinsohn, J. and Swanson, J. A. (2007). Differential association of phosphatidylinositol 3-kinase, SHIP-1, and PTEN with forming phagosomes. *Mol. Biol. Cell* **18**, 2463-2472.

Kerr, M. C. and Teasdale, R. D. (2009). Defining macropinocytosis. *Traffic* **10**, 364-371.

Kholodenko, B. N., Hancock, J. F. and Kolch, W. (2010). Signalling ballet in space and time. *Nat. Rev. Mol. Cell Biol.* **11**, 414-426.

Knapp, P. E. and Swanson, J. A. (1990). Plasticity of the tubular lysosomal compartment in macrophages. *J. Cell Sci.* **95**, 433-439.

Krauß, M. and Haucke, V. (2007). Phosphoinositides: regulators of membrane traffic and protein function. *FEBS Lett.* **581**, 2105-2111.

Lanzetti, L., Palamidessi, A., Areces, L., Scita, G. and Di Fiore, P. P. (2004). Rab5 is a signalling GTPase involved in actin remodelling by receptor tyrosine kinases. *Nature* **429**, 309-314.

Larsen, E. C., Ueyama, T., Brannock, P. M., Shirai, Y., Saito, N., Larsson, C., Loegering, D., Weber, P. B. and Lennartz, M. R. (2002). A role for PKC-ε in FcγR-mediated phagocytosis by RAW 264.7 cells. *J. Cell Biol.* **159**, 939-944.

Lemmon, M. A., Ferguson, K. M., O'Brien, R., Sigler, P. B. and Schlessinger, J. (1995). Specific and high-affinity binding of inositol phosphates to an isolated pleckstrin homology domain. *Proc. Natl. Acad. Sci. USA* **92**, 10472-10476.

Mercer, J. and Helenius, A. (2009). Virus entry by macropinocytosis. *Nat. Cell Biol.* **11**, 510-520.

Oancea, E., Teruel, M. N., Quest, A. F. G. and Meyer, T. (1998). Green fluorescent protein (GFP)-tagged cysteine-rich domains from protein kinase C as fluorescent indicators for diacylglycerol signaling in living cells. *J. Cell Biol.* **140**, 485-498.

Palamidessi, A., Frittoli, E., Garré, M., Faretta, M., Mione, M., Testa, I., Diaspro, A., Lanzetti, L., Scita, G. and Di Fiore, P. P. (2008). Endocytic trafficking of Rac is required for the spatial restriction of signaling in cell migration. *Cell* **134**, 135-147.

Porat-Shliom, N., Kloog, Y. and Donaldson, J. G. (2008). A unique platform for H-Ras signaling involving clathrin-independent endocytosis. *Mol. Biol. Cell* **19**, 765-775.

Prior, I. A., Muncke, C., Parton, R. G. and Hancock, J. F. (2003). Direct visualization of Ras proteins in spatially distinct cell surface microdomains. *J. Cell Biol.* **160**, 165-170.

Rameh, L. E., Arvidsson, A., Carraway, K. L., 3rd, Couvillon, A. D., Rathbun, G., Crompton, A., VanRenterghem, B., Czech, M. P., Ravichandran, K. S., Burakoff, S. J. et al. (1997). A comparative analysis of the phosphoinositide binding specificity of pleckstrin homology domains. *J. Biol. Chem.* **272**, 22059-22066.

Rodrigues, G. A., Falasca, M., Zhang, Z., Ong, S. H. and Schlessinger, J. (2000). A novel positive feedback loop mediated by the docking protein Gab1 and phosphatidylinositol 3-kinase in epidermal growth factor receptor signaling. *Mol. Cell. Biol.* **20**, 1448-1459.

Sun, P., Yamamoto, H., Suetsugu, S., Miki, H., Takenawa, T. and Endo, T. (2003). Small GTPase Rah/Rab34 is associated with membrane ruffles and macropinosomes and promotes macropinosome formation. *J. Biol. Chem.* **278**, 4063-4071.

Swanson, J. A. (1989). Phorbol esters stimulate macropinocytosis and solute flow through macrophages. *J. Cell Sci.* **94**, 135-142.

Swanson, J. A. (2008). Shaping cups into phagosomes and macropinosomes. *Nat. Rev. Mol. Cell Biol.* **9**, 639-649.

Swanson, J. A. and Watts, C. (1995). Macropinocytosis. *Trends Cell Biol.* **5**, 424-428.

Swanson, J. A., Johnson, M. T., Beningo, K., Post, P., Mooseker, M. and Araki, N. (1999). A contractile activity that closes phagosomes in macrophages. *J. Cell Sci.* **112**, 307-316.

Várnai, P., Rother, K. I. and Balla, T. (1999). Phosphatidylinositol 3-kinase-dependent membrane association of the Bruton's tyrosine kinase pleckstrin homology domain visualized in single living cells. *J. Biol. Chem.* **274**, 10983-10989.

Vieira, O. V., Botelho, R. J., Rameh, L., Brachmann, S. M., Matsuo, T., Davidson, H. W., Schreiber, A., Backer, J. M., Cantley, L. C. and Grinstein, S. (2001). Distinct roles of class I and class III phosphatidylinositol 3-kinases in phagosome formation and maturation. *J. Cell Biol.* **155**, 19-25.

Welliver, T. P., Chang, S. L., Linderman, J. J. and Swanson, J. A. (2011). Ruffles limit diffusion in the plasma membrane during macropinosome formation. *J. Cell Sci.* **124**, 4106-4114.

Yoshida, S., Hoppe, A. D., Araki, N. and Swanson, J. A. (2009). Sequential signaling in plasma-membrane domains during macropinosome formation in macrophages. *J. Cell Sci.* **122**, 3250-3261.

Zhang, Y., Hoppe, A. D. and Swanson, J. A. (2010). Coordination of Fc receptor signaling regulates cellular commitment to phagocytosis. *Proc. Natl. Acad. Sci. USA* **107**, 19332-19337.